Report

Current Biology

Male-Killing *Spiroplasma* Alters Behavior of the Dosage Compensation Complex during *Drosophila melanogaster* Embryogenesis

Highlights

- The DCC becomes mis-localized in *Spiroplasma*-infected male fruit fly embryos
- Infected males exhibit ectopic H4K16 acetylation and genome-wide gene mis-expression
- Infection leads to death of females artificially expressing the DCC

Authors

Becky Cheng, Nitin Kuppanda, John C. Aldrich, Omar S. Akbari, Patrick M. Ferree

Correspondence

omar.akbari@ucr.edu (O.S.A.), pferree@kecksci.claremont.edu (P.M.F.)

In Brief

Cheng et al. show that infection of the fruit fly with a male-killing *Spiroplasma* strain causes mis-localization of the dosage compensation complex (DCC) and abnormal gene expression in young male embryos, and death of females artificially expressing low levels of this complex. The bacterium may therefore target the DCC directly to kill males.

Cheng et al., 2016, Current Biology *26*, 1–7
May 23, 2016
http://dx.doi.org/10.1016/j.cub.2016.03.050

CellPress

Please cite this article in press as: Cheng et al., Male-Killing *Spiroplasma* Alters Behavior of the Dosage Compensation Complex during *Drosophila melanogaster* Embryogenesis, Current Biology (2016), http://dx.doi.org/10.1016/j.cub.2016.03.050

Current Biology
Report

Male-Killing *Spiroplasma* Alters Behavior of the Dosage Compensation Complex during *Drosophila melanogaster* Embryogenesis

Becky Cheng,[1] Nitin Kuppanda,[1] John C. Aldrich,[1] Omar S. Akbari,[2,*] and Patrick M. Ferree[1,*]
[1]W.M. Keck Science Department, Claremont McKenna, Pitzer and Scripps Colleges, 925 N. Mills Avenue, Claremont, CA 91711, USA
[2]Department of Entomology and Riverside Center for Disease Vector Research, Institute for Integrative Genome Biology, University of California, Riverside, Riverside, CA 92521, USA
*Correspondence: omar.akbari@ucr.edu (O.S.A.), pferree@kecksci.claremont.edu (P.M.F.)
http://dx.doi.org/10.1016/j.cub.2016.03.050

SUMMARY

Numerous arthropods harbor maternally transmitted bacteria that induce the preferential death of males [1–7]. This sex-specific lethality benefits the bacteria because males are "dead ends" regarding bacterial transmission, and their absence may result in additional resources for their viable female siblings who can thereby more successfully transmit the bacteria [5]. Although these symbionts disrupt a range of developmental processes [8–10], the underlying cellular mechanisms are largely unknown. It was previously shown that mutations in genes of the dosage compensation pathway of *Drosophila melanogaster* suppressed male killing caused by the bacterium, *Spiroplasma* [10]. This result suggested that dosage compensation is a target of *Spiroplasma*. However, it remains unclear how this pathway is affected, and whether the underlying interactions require the male-specific cellular environment. Here, we investigated the cellular basis of male embryonic lethality in *D. melanogaster* induced by *Spiroplasma*. We found that the dosage compensation complex (DCC), which acetylates X chromatin in males [11], becomes mis-localized to ectopic regions of the nucleus immediately prior to the killing phase. This effect was accompanied by inappropriate histone acetylation and genome-wide mis-regulation of gene expression. Artificially induced formation of the DCC in infected females, through transgenic expression of the DCC-specific gene *msl-2*, resulted in mis-localization of this complex to non-X regions and early *Spiroplasma*-induced death, mirroring the killing effects in males. These findings strongly suggest that *Spiroplasma* initiates male killing by targeting the dosage compensation machinery directly and independently of other cellular features characteristic of the male sex.

RESULTS AND DISCUSSION

Spiroplasma are cell-wall-less spirochetes belonging to the bacterial Mollicute class that infect the hemolymph and egg cytoplasm of their insect hosts [12, 13]. Male-killing strains of *Spiroplasma* are common within the *Drosophila* genus, having been detected in at least eight different *Drosophila* species including *D. melanogaster* [6]. In this latter species, males, but not females, infected with the male-killing MSRO (for *melanogaster* sex ratio organism) strain of *Spiroplasma* exhibit disrupted CNS formation and heightened apoptosis in epithelial cells during the middle stages of embryogenesis, and they fail to reach the larval stages [14, 15]. Previous work has suggested that *Spiroplasma* induces developmental defects in males by altering the male-specific process of dosage compensation [10]. In these studies, genetic crosses were utilized to test whether strong loss-of-function mutations in several male specific lethal (*msl*) genes, including *msl-1*, *msl-2*, and *msl-3*, as well as *maleless* (*mle*), and *male absent on the first* (*mof*), could modulate male killing [10]. Normally *msl-2* is expressed only in males while the other genes are expressed in both sexes. In males the MSL-2 protein associates with the other proteins to form the dosage compensation complex (DCC) (also known as the MSL complex), which localizes preferentially to specific regions within the gene-containing euchromatin of the single X [16, 17]. The presence of this complex induces acetylation of histone H4 at lysine residue 16 (H4K16ac) within the body of compensated genes as a result of MOF acetylase activity [11, 18, 19]. This modification is accompanied by an ~2-fold transcriptional increase of most genes on the X chromosome so that the X-to-autosome (non-sex chromosome) ratio for gene expression in males matches that found in females, which have two active X chromosomes [20]. A substantial portion of *Spiroplasma*-infected males mutant for any of the DCC components were found to survive past the embryonic male-killing phase [10]. This result demonstrated a genetic interaction between the dosage compensation components and the level of male killing. However, it remains to be determined whether this effect reflects a direct bacterial targeting of the dosage compensation machinery or instead an indirect suppression of male killing, perhaps because dosage compensation is downstream of another targeted cellular process.

To better understand this phenomenon, we cytologically examined the subcellular behavior of the DCC and its

Table 1. Adult Sex Ratios for *Spiroplasma*-Infected and Uninfected Fly Lines

Fly Line	Number Females	Number Males	Total	Percent Males
Canton-S	117	99	216	46
Canton-S (Sp+)	178	0	178	0
w;msl-3-GFP	233	248	481	52
w;msl-3-GFP (Sp+)	265	5	270	2

histone acetylation mark just before the lethal phase in male *D. melanogaster* embryos infected with MSRO *Spiroplasma* (from here onward referred to as *Spiroplasma*) [14]. This strain was lethal to ≥96% of male progeny in the *D. melanogaster* lines used in this study (Table 1). In control (uninfected) embryos, very little DCC signal was seen before 3 hr after egg deposition (AED), as indicated by hardly detectable levels of visible MOF or H4K16ac on chromatin (n = 7 embryos; Figure 1A), consistent with previous studies showing that DCC formation occurs around this time [21, 22]. By 4–6 hr AED, during embryonic germband extension, MOF appeared as a distinct sub-nuclear focus that was highly enriched with H4K16ac within the epithelial (outer) cells of male embryos (n = 13 embryos; Figure 1B). This enrichment of H4K16ac also co-localized with a single bright region of MSL-3 (n = 11 embryos; Figure S1) and resided immediately adjacent to or overlapping with X sequences (Figure S2). These signals became strongest and evenly distributed across the embryo's surface by the beginning of segmentation (7+ hr AED) (Figures 1C and S1).

In *Spiroplasma*-infected male embryos, very little MOF and H4K16ac signals were visible before 3 hr AED (n = 6 embryos), similar to control male embryos at this time (Figure 1D, compared to Figure 1A). At 4–6 hr AED, MOF and H4K16ac accumulated into sub-nuclear foci corresponding to X sequences within a portion of nuclei (n = 15 embryos; Figure 1E). However, these signals only weakly accumulated into foci or not at all, and in many regions of the embryo they were distributed broadly across the nucleus (n = 13 of 15 embryos; Figure 1E). In contrast, overall nuclear morphology appeared normal in most cells at this time, although a small portion of nuclei appear hyper-condensed (Figure 1E). By 9+ hr AED, when embryos undergo body segmentation, many nuclei exhibited abnormal hyper-condensation (Figure 1F). Additionally, DCC and H4K16ac signals became very low (n = 15 embryos; Figures 1F and S1), which may stem from general chromatin mis-organization as nuclear morphology became more abnormal. No DCC foci were observed in wild-type *Spiroplasma*-infected or uninfected female embryos (n = 9 embryos; Figure S3), and, consistent with previous studies [14, 15], all were normal in cellular morphology.

The observation of DCC localization and H4K16 acetylation in ectopic nuclear regions led us to ask whether this effect causes abnormal genome-wide mis-regulation of gene expression, which could explain defective male development. In order to address this question, we collected male enriched embryo broods (see the Supplemental Experimental Procedures) at both 2–3 and 5–6 hr AED and performed transcriptional profiling of total mRNAs extracted from these samples (Table S1). Although there was a high congruence of gene expression between control and infected embryos, a subset of genes appeared to be mis-expressed with a bias toward overexpression in infected embryos at both developmental times (Figure 2A; Table S1). To further evaluate this trend, we plotted the distribution of expression ratios (infected/uninfected) for autosomal and X-linked genes at both time points and used the Kolmogorov-Smirnov (K-S) test to determine an overall deviation from a 1:1 ratio (i.e., no change in expression between conditions). The distribution of X-linked expression ratios significantly deviated at 2–3 hr AED ($p < 1 \times 10^{-4}$), while the autosomal distribution was found to significantly deviate at both 2–3 and 5–6 hr AED ($p < 1 \times 10^{-7}$ and $p < 1 \times 10^{-4}$, respectively; Table S1), confirming the observed bias toward global overexpression (Figure 2A).

Closer inspection of our datasets revealed that a modest number of both X and autosomal (non-sex chromosome) genes were significantly mis-expressed at each developmental time (Figures 2B and 2C; Table S1), although this number may be underestimated due to large variation in expression between replicates, potentially reflecting the stochastic nature of DCC mis-localization. Mis-expressed genes were located across each chromosome and not clustered at distinct region(s) (Figure 2B), consistent with the observed lack of DCC concentration at distinct non-X regions (Figures 1E and 1F). The finding of overexpressed genes on the X, however, was surprising given that the DCC normally becomes enriched on X chromatin, and overall loss of DCC there would be expected to result in the opposite pattern. These findings are consistent with previous studies showing that dissociation of the DCC from the male X results in MOF localization and H4K16 acetylation across the genome, as well as upregulation of autosomal genes, but not X-linked genes [23, 24]. The majority of mis-expressed genes were overexpressed at both developmental times (Figures 2B and 2C; Table S1), consistent with the H4K16ac mark being associated with increased gene expression [25]. A portion of mis-expressed genes on the X and the autosomes exhibited greater than 2-fold expression level differences in infected embryos (Figure 2C), when, under normal conditions, the DCC transcriptionally compensates at only an ~2-fold level expression change on the X. These patterns may reflect an abnormal chromatin remodeling behavior of the DCC in the presence of *Spiroplasma*. This idea is consistent with previous studies suggesting that DCC activity is normally constrained by an unknown mechanism so that X gene upregulation occurs at an ~2-fold level [24, 26, 27]; it is possible that the male-killing effect alleviates this constraint so that the DCC becomes hyperactive. Alternatively, higher than 2-fold expression changes may also occur from mis-regulation of loci involved in transcriptional repression.

Some genes were consistently mis-expressed at both 2–3 and 5–6 hr AED (Figure 2D; Table S1). These genes represent a range of biological functions, with those involved cuticle formation being one of the more highly represented groups (Figure S4; Table S1). These genes, and other—such as those involved in muscle assembly—are normally not expressed until late embryogenesis and afterward, suggesting that ectopic DCC mis-localization leads to activation of genes that are not normally expressed at these earlier times. While many of these genes may become mis-expressed due to ectopic DCC activity, others including the immune genes IM1, IM2-3, and IM4 (Table S1) could be induced as a general response to

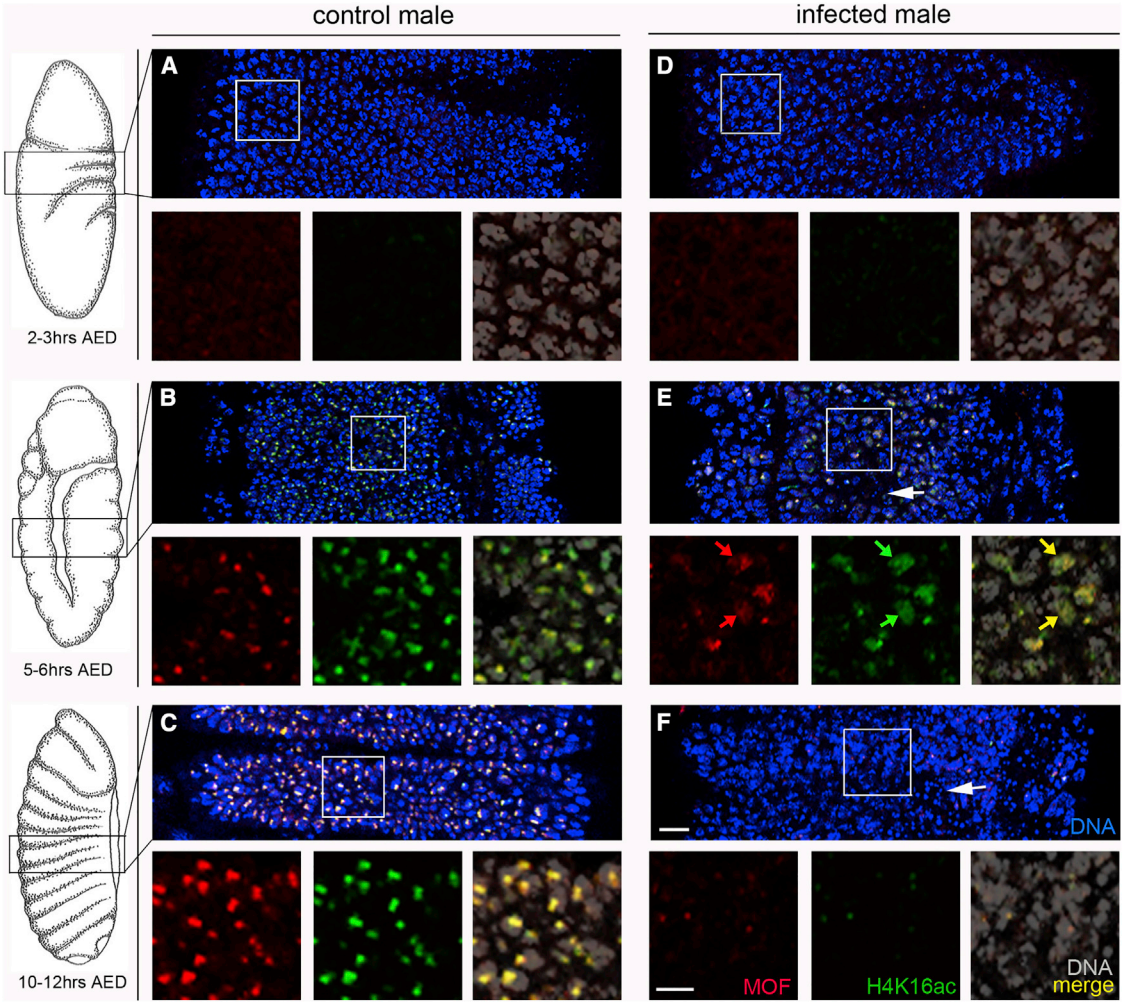

Figure 1. *Spiroplasma*-Infected Male Embryos Exhibit Mis-localized MOF and H4K16ac

Each panel (A–F) shows a horizontal slice across the middle region of an embryo and a region (white box) shown in a higher magnification with fluorescence channels separated into three square panels below.

(A and B) Both control (uninfected) and infected embryos at 2–3 hr after egg deposition (AED) show very little MOF or H4K16ac signals.

(C and D) At 5–6 hr AED, MOF and H4K16ac signals become bright and co-localize to a single focus in each nucleus of control embryos. The H4K16ac signals co-localizes with X sequences and overlap with MSL3 (see Figures S1 and S2, respectively). In contrast, these signals, although still overlapping, become distributed across nuclei in infected embryos (yellow arrows in right panel). Some nuclei in infected embryos appear hyper-condensed (white arrow).

(E and F) At 9–11 hr AED, MOF and H4K16ac signals persist as bright foci in the nuclei of control embryos. However, in infected embryos these signals are barely visible in most nuclei, and more nuclei are hyper-condensed (white arrow). Scale bar, 15 μm in the top panel and 5 μm in the high-magnification bottom panels (F).

bacterial infection. The majority of immune response genes, however, were not induced at either developmental time analyzed (Table S1), a pattern that is consistent with previous work suggesting that *Spiroplasma* is capable of largely evading the host's immune system [28]. Of particular interest were two overexpressed regulators of apoptosis, *reaper* and *sickle*, at 2–3 hr AED, and just *sickle* at 5–6 hr AED (Table S1). The nature of our data does not allow us to address whether increased expression of these genes is a direct result of DCC mis-localization or instead a secondary response to broad gene mis-regulation. Nevertheless, elevated expression of these genes is consistent with previous cytological detection of increased cell death due to *Spiroplasma* infection at later embryonic stages [15].

Based on the above observations, *Spiroplasma* may initiate male killing by directly altering DCC localization as it forms during early embryogenesis, thereby leading to wide-scale gene mis-expression and developmental abnormalities. Although DCC-directed compensation is a distinguishing characteristic of the male sex during early development, other sex-specific differences exist at this time [29–31]. It is possible that *Spiroplasma* targets an earlier male-specific factor or process that leads to DCC mis-behavior or, alternatively, that other male factors could be essential for DCC targeting; either of these scenarios is consistent with suppression of male killing by mutational loss of the DCC [10]. To test whether the DCC is the sole male-specific factor required for male killing, we assessed the viability of *Spiroplasma*-infected *D. melanogaster* females artificially

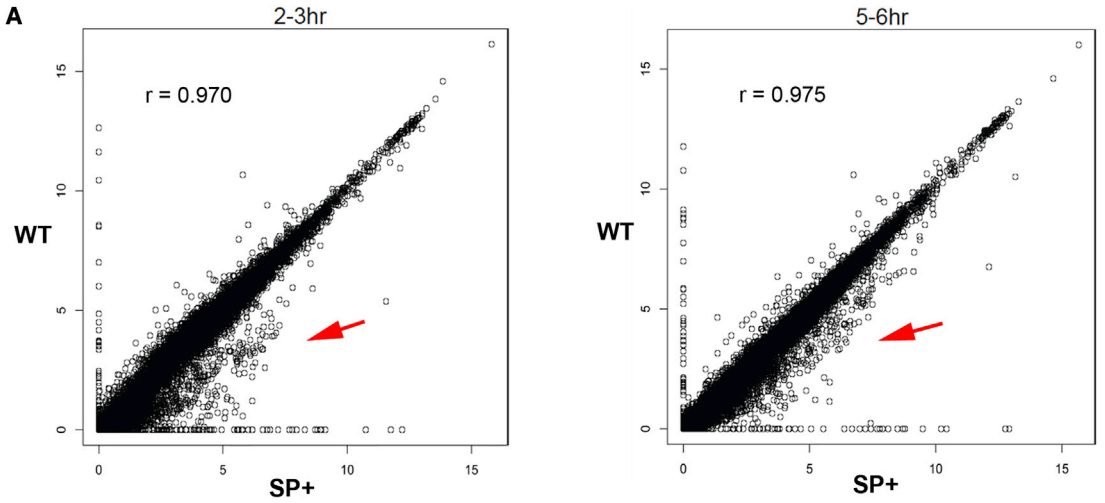

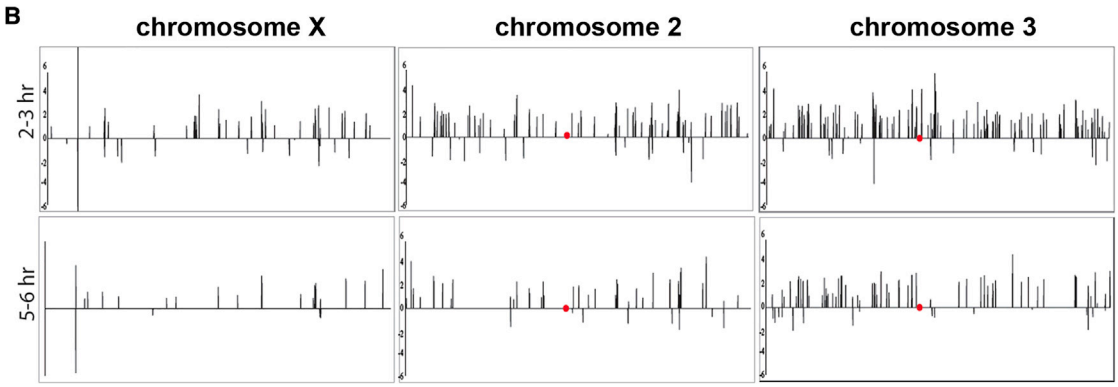

C

	2-3hr		5-6hr	
	X-linked	Autosomal	X-linked	Autosomal
off to on	6	38	0	6
< 2 fold up	8	24	13	55
≥ 2 fold up	26	200	6	60
unchanged	2311	12509	2336	12633
< 2 fold down	8	15	0	9
≥ 2 fold down	1	10	0	1
on to off	1	9	0	1
total	2354	12758	2355	12758

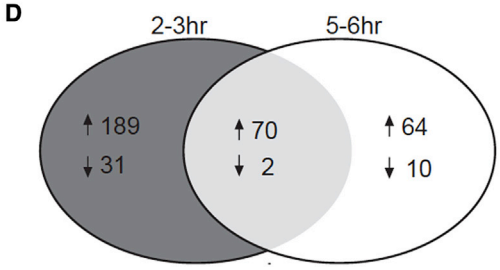

Figure 2. *Spiroplasma*-Infected Male Embryos Exhibit Genome-wide Mis-regulation of Gene Expression

(A) Scatterplots show averaged FPKM values between corresponding replicates for expressed genes in wild-type embryos plotted against those of *Spiroplasma*-infected embryos for both time points. Values are shown in log scale. Red arrow indicates a higher clustering of genes that appear overexpressed in infected embryos.

(B) Chromosome maps depicting the positions of significantly mis-expressed genes in *Spiroplasma*-infected embryos relative to uninfected embryos. Peaks above the horizontal lines represent genes that are significantly overexpressed in *Spiroplasma*-infected embryos, and peak height reflects expression ratio on the log scale. Red dot corresponds to the chromosome centromeres.

(C) The number of significantly mis-expressed genes on the X versus the autosomes (non-sex chromosomes) and their general fold change values between *Spiroplasma*-infected and uninfected embryos. The patterns in (B) and (C) reflect an enrichment of overexpressed genes on all chromosomes and for both developmental times.

(D) A Venn diagram depicting the number of overexpressed genes (up arrow) and under-expressed (down arrow) in *Spiroplasma*-infected embryos that are unique to each developmental time point and those common between these times.

See Table S1 for raw data and Figure S4 for ontogeny groupings of mis-expressed genes common between 2–3 and 5–6 hr AED.

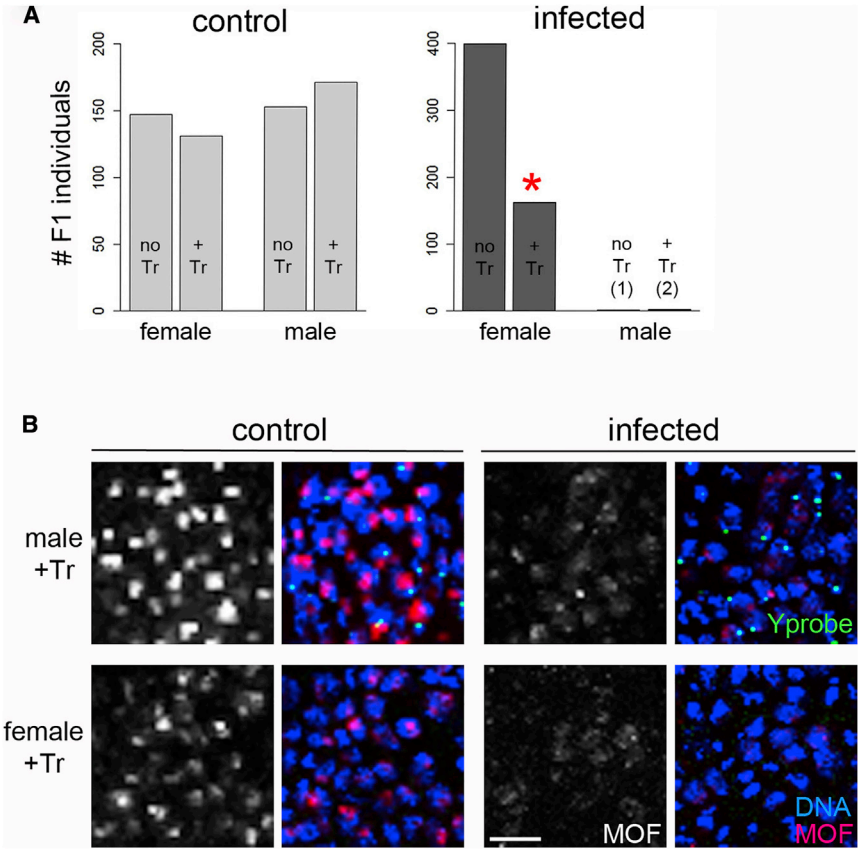

Figure 3. *Spiroplasma* Infection Causes Death of Females Expressing Low Levels of MSL-2 and Mis-localized DCC during Female Embryogenesis

(A) The number of F1 progeny carrying the *hsp83-MSL-2* transgene (+Tr) and their siblings without the transgene (no Tr) produced from either uninfected (control) or *Spiroplasma*-infected mothers. Red asterisk indicates a significant difference between transgenic and non-transgenic females infected by *Spiroplasma*.

(B) Transgenic male and female embryos that are either uninfected or *Spiroplasma* infected. Uninfected embryos of both sexes show distinct MOF localization, whereas in infected embryos MOF fails to concentrate and becomes distributed lightly across nuclei. Non-transgenic females do not exhibit foci of MOF or H4K16ac (see Figure S3). Scale bar, 5 μm.

expressing *msl-2* via a heat-shock-inducible *hsp83* promoter [17]. Under heat shock, this transgene expresses *msl-2* at a high level, an effect that is strongly lethal to females due to a proportionally high level of DCC formation and activity [17]. However, without heat shock this transgene is leaky, expressing a low level of *msl-2* that does not affect female viability when in a genetic background that is heterozygous for an *msl-1* mutation [17]. DCC formation through leaky expression of this transgene was previously shown in female salivary gland nuclei [17]. Here, we observed single foci of MOF in the nuclei of female embryos carrying one transgene copy (Figure 3), demonstrating that this transgene is also active during early development.

To assess the effect of DCC formation on the viability of infected females, we crossed uninfected males carrying one copy of the *hsp83 msl-2* transgene to wild-type females that were either *Spiroplasma* infected or uninfected and scored the viability of the resulting offspring (see the Experimental Procedures for details of the crosses and genotypes). The ratio of uninfected, transgenic to uninfected, non-transgenic female progeny was close to 1 (chi-square goodness-of-fit test, $p = 0.55$) (Figure 3A), recapitulating that the leaky expression of the *msl-2* transgene alone has very little effect on female viability when in an *msl-1* heterozygous mutant background. However, the ratio of infected, transgenic to infected, non-transgenic female progeny was 0.411 (Figure 3A), a highly significant deviation from the expected 1:1 ratio of these genotypes that occurred in the absence of infection (chi-square goodness-of-fit test, $p < 0.0001$). Thus, the presence of the DCC is lethal to female embryos only when they carry the *Spiroplasma* infection. Consistent with this finding, *Spiroplasma*-infected female embryos expressing *msl-2* were nearly identical in abnormal sub-cellular phenotype to those of wild-type infected male embryos: they exhibited mis-localized MOF at 4+ hr AED, and these signals diminished in intensity as nuclear morphology degenerated during later developmental times (Figure 3B). In contrast, transgene-carrying female embryos without infection showed well-formed MOF foci and normal nuclear morphology (Figure 3B).

Although compensation of most X-linked genes involves the DCC, a sub-set of genes involved in early embryogenesis become compensated as much as 1 hr before DCC formation, thus likely occurring through a DCC-independent mechanism [31]. Although the details of this process are currently unknown, it is clear that gene dosage compensation in *Drosophila* is more complex than previously thought and extends beyond the DCC pathway. Moreover, this complexity infers that the embryonic cytotype begins to differ substantially between males and females as early as 1 hr after fertilization. Our ability to reconstitute the killing effect in female embryos by expression of *msl-2* alone strongly suggests that DCC mis-localization is a direct effect of *Spiroplasma* and does not result secondarily from targeting of the earlier, DCC-independent compensation. More generally, DCC mis-localization by *Spiroplasma* does not require interactions with other cellular processes that are characteristic of male embryos. Thus, DCC mis-localization can be viewed as a sex-independent phenomenon that may arise from a specific interaction of this complex with a bacterium-produced factor in the cells of whichever sex these components are present. This interaction could also involve other host cellular components that must be present in both male and female embryos.

Taken together, our results support a model in which *Spiroplasma* initiates male killing by altering DCC behavior on both the X and ectopically on non-sex chromosomes, thereby leading to abnormal histone acetylation and gene mis-expression across

the genome. The mis-expression of certain genes—such as those involved in apoptosis—may elicit severe cellular responses at even slightly elevated levels [32, 33]. Thus, perturbations of several key genes may have profound deleterious effects on early male development. Wild-type infected females would be spared this effect because these individuals do not normally express the MSL-2 protein and, therefore, harbor no integral DCC [17, 34]. Knowledge that the DCC itself may be a direct target of *Spiroplasma* in *D. melanogaster* will help to identify the specific interacting molecules of host and symbiont that underlie this phenomenon through further experimentation.

EXPERIMENTAL PROCEDURES

Fly Lines and Infection

Embryo collections for cytology were obtained from two different fly lines. One was a *Canton-S* line carrying the MSRO strain of *Spiroplasma* that was used previously in [14]. A second was a line homozygous for a transgenic copy of *msl-3-GFP* (a gift from M. Kuroda). This line was infected for this particular study by hemolymph transfer from the infected *Canton-S* line (protocol provided by T. Haselkorn). Fly lines were propagated by crossing virgin infected females from each fly line to males from an uninfected stock of the same genetic background. Before crossing, infected females were held to 1 week in order to insure strong penetrance of male killing. All embryo collections, crosses, and propagation lines were maintained at 25°C.

For testing the effects of *msl-2* expression in infected females, we crossed *w; msl-1; P{w$^+$ hsp83-msl-2}* females (stock obtained from M. Kuroda) to *w / Y; +; TM3 Ser Sb / TM6 Tub* males. F1 Male progeny of the genotype *w / Y; msl-1 / +; P{w$^+$ hsp83-msl-2} / TM3 Ser Sb* were then crossed to either *Spiroplasma*-infected or uninfected *Canton-S* females aged 1 week. The resulting progeny from this cross carried either the *P{w+ hsp83-msl-2}* transgene or the *TM3 Ser Sb* balancer chromosome and were easily distinguished by the presence or absence of the two co-inherited dominant markers.

Embryo Collection and Fixation

Mated females of the desired genotype and infection status were allowed to lay on collection plates containing grape agar medium, and embryos were aged to the desired developmental stage at 25°C. Embryos were dechorionated in 50% bleach, fixed for 10 min in 4% paraformaldehyde/heptane, and devitellinized in methanol. Embryos were either kept in methanol at −20°C for long-term storage or rehydrated for cytolological purposes. Hydration was conducted in a series of methanol:water solutions in order of the following ratios: 9:1, 5:5, and 1:9, followed by three 5-min washes in 1 × PBT (1 × PBS and 0.1% Tween 20).

Immunohistochemical Staining and Fluorescence In Situ Hybridization

Hydrated, fixed embryos were incubated in the following primary antibodies overnight at 4°C: mouse anti-GFP (1:50, clone number 4C9, Developmental Studies Hybridoma Bank); goat anti-MOF (1:100, clone number dn-17, Santa Cruz Biotechnology); and rabbit anti-acetyl-histone H4 lysine 16 (1:100, catalog number 07-329, Millipore). Following incubation with primary antibodies, embryos were washed 3 × 15 min in 1 × PBT before secondary antibody staining. Anti-mouse, anti-rabbit, and anti-goat secondary antibodies were conjugated with either Alexa 555 or Alexa 633 (Molecular Probes-Invitrogen) and used at a dilution of 1:300. Secondary staining was conducted out of light for 1 hr at room temperature and washed three times subsequently.

Fluorescence in situ hybridization was conducted with an oligonucleotide probe specific for a satellite DNA sequence unique to the Y chromosome [35]. The probe consisted of the sequence 5′-AAT ACA ATA CAA TAC AAT ACA ATA CAA TAC-3′ and was synthesized commercially (IDT) with Cy2 conjugated at the 5′ end. Whole-mount embryo hybridizations were conducted as described [35], except that embryos used for this purpose were stained first with antibodies, re-fixed in 4% paraformaldehyde for 45 min, and washed three times in 2 × saline-sodium citrate and Tween-20 (SSCT) buffer before probe hybridization.

Confocal Imaging and Data Processing

Fluorescence images were collected on a Leica TCS SPE confocal microscope. Images were collected by using identical laser, gain, and offset settings for both uninfected and infected tissues for direct comparison between these conditions. The specific setting values of the original Leica-formatted images can be obtained at request from the authors. After image capture, image files were exported in TIFF format and processed in Adobe Photoshop CS5 v.12. Images were enhanced with the brightness and contrast settings being manipulated identically between infected and uninfected conditions.

ACCESSION NUMBERS

The accession number for the RNA sequence reported in this paper is SRA: PRJNA318373.

SUPPLEMENTAL INFORMATION

Supplemental Information includes Supplemental Experimental Procedures, four figures, and one table and can be found with this article online at http://dx.doi.org/10.1016/j.cub.2016.03.050.

AUTHOR CONTRIBUTIONS

B.C. performed the cytological experiments and genetic crosses. N.K. performed the genetic crosses. O.S.A. performed the transcriptomic analyses and statistical tests. J.C.A., O.S.A., and P.M.F. analyzed the data. P.M.F. and O.S.A. designed the experiments. P.M.F. and J.C.A. wrote the manuscript. All authors have discussed the results and contributed to the manuscript.

ACKNOWLEDGMENTS

We thank M. Kuroda for the *w; msl-1*; *P{w+ hsp83-msl-2}* and *w*; *msl-3-GFP* fly lines, C. Staber for the SD fly lines, C.-T. Wu and D. Colognori for the X16E FISH probe, and T. Hazelkorn for the hemolymph transfer protocol. We also thank B. Hay, E. Ferree, V. Meller, and J. Birchler for helpful input. This study was supported by an NSF CAREER award (NSF1451839) to P.M.F., an NIH Career Transition Award (K22) (5K22AI113060-02) to O.S.A., and a USDA National Institute of Food and Agriculture, Hatch project 1009509 to O.S.A.

Received: February 5, 2016
Revised: March 16, 2016
Accepted: March 21, 2016
Published: May 5, 2016

REFERENCES

1. Werren, J.H., Skinner, S.W., and Huger, A.M. (1986). Male-killing bacteria in a parasitic wasp. Science *231*, 990–992.
2. Zeh, D.W., Zeh, J.A., and Bonilla, M.M. (2005). Wolbachia, sex ratio bias and apparent male killing in the harlequin beetle riding pseudoscorpion. Heredity (Edinb) *95*, 41–49.
3. Jiggins, F.M., Hurst, G.D., Schulenburg, J.H., and Majerus, M.E. (2001). Two male-killing Wolbachia strains coexist within a population of the butterfly Acraea encedon. Heredity (Edinb.) *86*, 161–166.
4. Werren, J.H., Hurst, G.D.D., Zhang, W., Breeuwer, J.A.J., Stouthamer, R., and Majerus, M.E. (1994). Rickettsial relative associated with male killing in the ladybird beetle (Adalia bipunctata). J. Bacteriol. *176*, 388–394.
5. Hurst, G.D., and Jiggins, F.M. (2000). Male-killing bacteria in insects: mechanisms, incidence, and implications. Emerg. Infect. Dis. *6*, 329–336.
6. Haselkorn, T.S. (2010). The Spiroplasma heritable bacterial endosymbiont of Drosophila. Fly (Austin) *4*, 80–87.
7. Whitcomb, R.F. (1980). The genus Spiroplasma. Annu. Rev. Microbiol. *34*, 677–709.

8. Riparbelli, M.G., Giordano, R., Ueyama, M., and Callaini, G. (2012). Wolbachia-mediated male killing is associated with defective chromatin remodeling. PLoS ONE *7*, e30045.
9. Ferree, P.M., Avery, A., Azpurua, J., Wilkes, T., and Werren, J.H. (2008). A bacterium targets maternally inherited centrosomes to kill males in Nasonia. Curr. Biol. *18*, 1409–1414.
10. Veneti, Z., Bentley, J.K., Koana, T., Braig, H.R., and Hurst, G.D. (2005). A functional dosage compensation complex required for male killing in Drosophila. Science *307*, 1461–1463.
11. Gelbart, M.E., Larschan, E., Peng, S., Park, P.J., and Kuroda, M.I. (2009). Drosophila MSL complex globally acetylates H4K16 on the male X chromosome for dosage compensation. Nat. Struct. Mol. Biol. *16*, 825–832.
12. Herren, J.K., Paredes, J.C., Schüpfer, F., and Lemaitre, B. (2013). Vertical transmission of a Drosophila endosymbiont via cooption of the yolk transport and internalization machinery. MBio *4*, e00532-12.
13. Anbutsu, H., and Fukatsu, T. (2006). Tissue-specific infection dynamics of male-killing and nonmale-killing spiroplasmas in Drosophila melanogaster. FEMS Microbiol. Ecol. *57*, 40–46.
14. Martin, J., Chong, T., and Ferree, P.M. (2013). Male killing Spiroplasma preferentially disrupts neural development in the Drosophila melanogaster embryo. PLoS ONE *8*, e79368.
15. Harumoto, T., Anbutsu, H., and Fukatsu, T. (2014). Male-killing Spiroplasma induces sex-specific cell death via host apoptotic pathway. PLoS Pathog. *10*, e1003956.
16. Meller, V.H., Wu, K.H., Roman, G., Kuroda, M.I., and Davis, R.L. (1997). roX1 RNA paints the X chromosome of male Drosophila and is regulated by the dosage compensation system. Cell *88*, 445–457.
17. Kelley, R.L., Solovyeva, I., Lyman, L.M., Richman, R., Solovyev, V., and Kuroda, M.I. (1995). Expression of msl-2 causes assembly of dosage compensation regulators on the X chromosomes and female lethality in Drosophila. Cell *81*, 867–877.
18. Alekseyenko, A.A., Larschan, E., Lai, W.R., Park, P.J., and Kuroda, M.I. (2006). High-resolution ChIP-chip analysis reveals that the Drosophila MSL complex selectively identifies active genes on the male X chromosome. Genes Dev. *20*, 848–857.
19. Gilfillan, G.D., Straub, T., de Wit, E., Greil, F., Lamm, R., van Steensel, B., and Becker, P.B. (2006). Chromosome-wide gene-specific targeting of the Drosophila dosage compensation complex. Genes Dev. *20*, 858–870.
20. Gupta, V., Parisi, M., Sturgill, D., Nuttall, R., Doctolero, M., Dudko, O.K., Malley, J.D., Eastman, P.S., and Oliver, B. (2006). Global analysis of X-chromosome dosage compensation. J. Biol. *5*, 3.
21. Rastelli, L., Richman, R., and Kuroda, M.I. (1995). The dosage compensation regulators MLE, MSL-1 and MSL-2 are interdependent since early embryogenesis in Drosophila. Mech. Dev. *53*, 223–233.
22. Franke, A., Dernburg, A., Bashaw, G.J., and Baker, B.S. (1996). Evidence that MSL-mediated dosage compensation in Drosophila begins at blastoderm. Development *122*, 2751–2760.
23. Bhadra, U., Pal-Bhadra, M., and Birchler, J.A. (1999). Role of the male specific lethal (msl) genes in modifying the effects of sex chromosomal dosage in Drosophila. Genetics *152*, 249–268.
24. Bhadra, M.P., Bhadra, U., Kundu, J., and Birchler, J.A. (2005). Gene expression analysis of the function of the male-specific lethal complex in Drosophila. Genetics *169*, 2061–2074.
25. Kind, J., Vaquerizas, J.M., Gebhardt, P., Gentzel, M., Luscombe, N.M., Bertone, P., and Akhtar, A. (2008). Genome-wide analysis reveals MOF as a key regulator of dosage compensation and gene expression in Drosophila. Cell *133*, 813–828.
26. Prestel, M., Feller, C., Straub, T., Mitlöhner, H., and Becker, P.B. (2010). The activation potential of MOF is constrained for dosage compensation. Mol. Cell *38*, 815–826.
27. Sun, L., Fernandez, H.R., Donohue, R.C., Li, J., Cheng, J., and Birchler, J.A. (2013). Male-specific lethal complex in Drosophila counteracts histone acetylation and does not mediate dosage compensation. Proc. Natl. Acad. Sci. USA *110*, E808–E817.
28. Herren, J.K., and Lemaitre, B. (2011). Spiroplasma and host immunity: activation of humoral immune responses increases endosymbiont load and susceptibility to certain Gram-negative bacterial pathogens in Drosophila melanogaster. Cell. Microbiol. *13*, 1385–1396.
29. Cline, T.W., and Meyer, B.J. (1996). Vive la différence: males vs females in flies vs worms. Annu. Rev. Genet. *30*, 637–702.
30. Schütt, C., and Nöthiger, R. (2000). Structure, function and evolution of sex-determining systems in Dipteran insects. Development *127*, 667–677.
31. Lott, S.E., Villalta, J.E., Schroth, G.P., Luo, S., Tonkin, L.A., and Eisen, M.B. (2011). Noncanonical compensation of zygotic X transcription in early Drosophila melanogaster development revealed through single-embryo RNA-seq. PLoS Biol. *9*, e1000590.
32. White, K., Tahaoglu, E., and Steller, H. (1996). Cell killing by the Drosophila gene reaper. Science *271*, 805–807.
33. Wing, J.P., Karres, J.S., Ogdahl, J.L., Zhou, L., Schwartz, L.M., and Nambu, J.R. (2002). Drosophila sickle is a novel grim-reaper cell death activator. Curr. Biol. *12*, 131–135.
34. Bashaw, G.J., and Baker, B.S. (1995). The msl-2 dosage compensation gene of Drosophila encodes a putative DNA-binding protein whose expression is sex specifically regulated by Sex-lethal. Development *121*, 3245–3258.
35. Ferree, P.M., and Barbash, D.A. (2009). Species-specific heterochromatin prevents mitotic chromosome segregation to cause hybrid lethality in Drosophila. PLoS Biol. *7*, e1000234.

Current Biology, Volume *26*

Supplemental Information

Male-Killing *Spiroplasma* Alters Behavior of the Dosage Compensation Complex during *Drosophila melanogaster* Embryogenesis

Becky Cheng, Nitin Kuppanda, John C. Aldrich, Omar S. Akbari, and Patrick M. Ferree

Figure S1

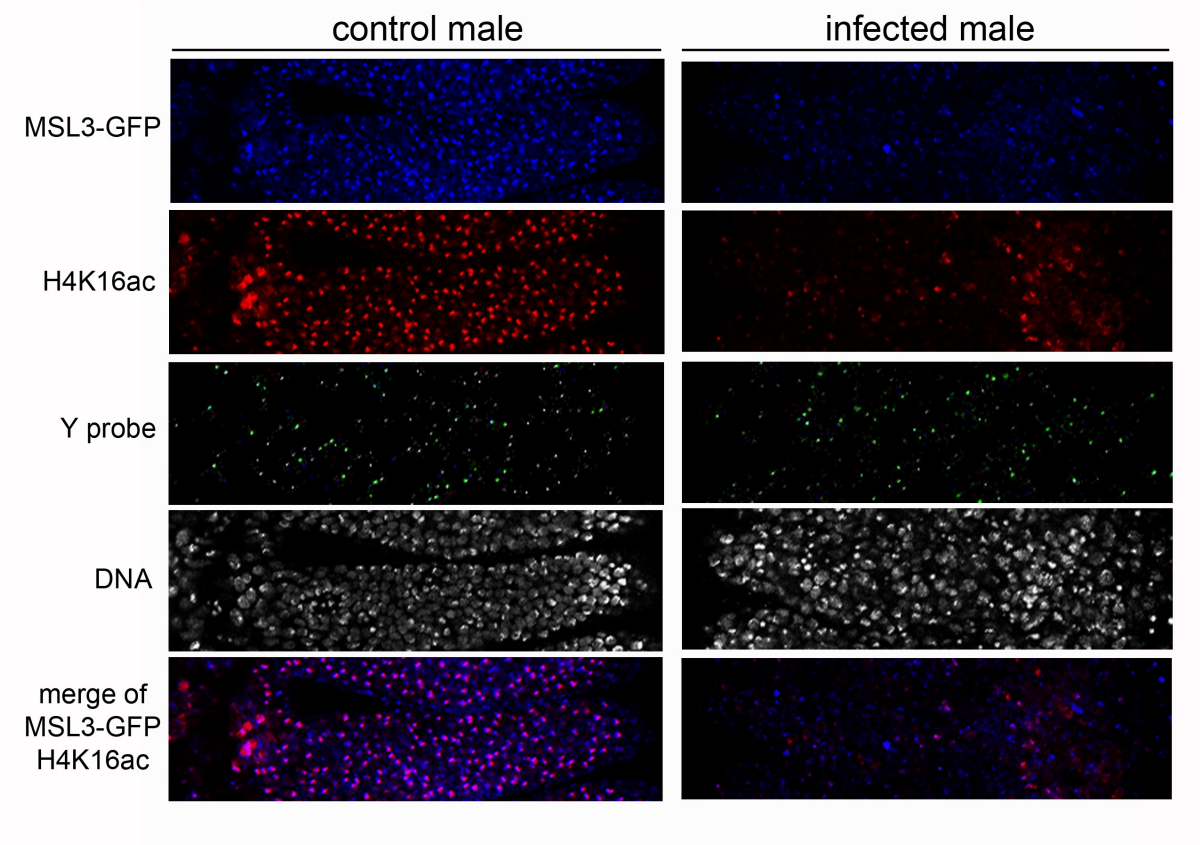

Figure S2

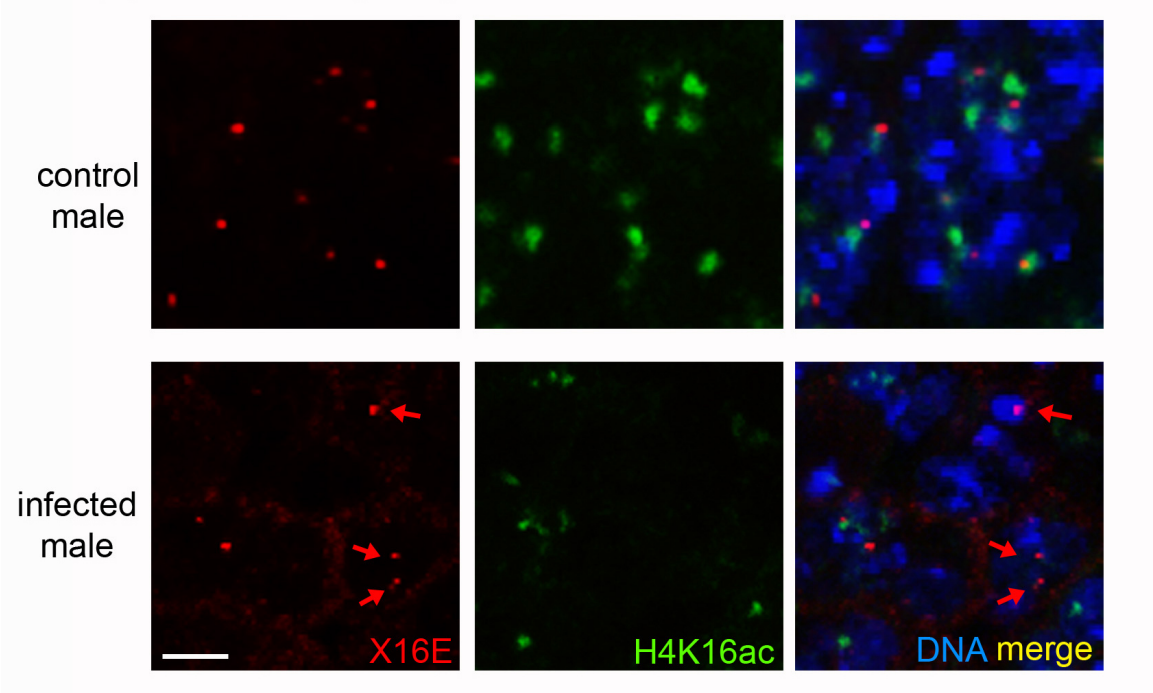

Figure S3

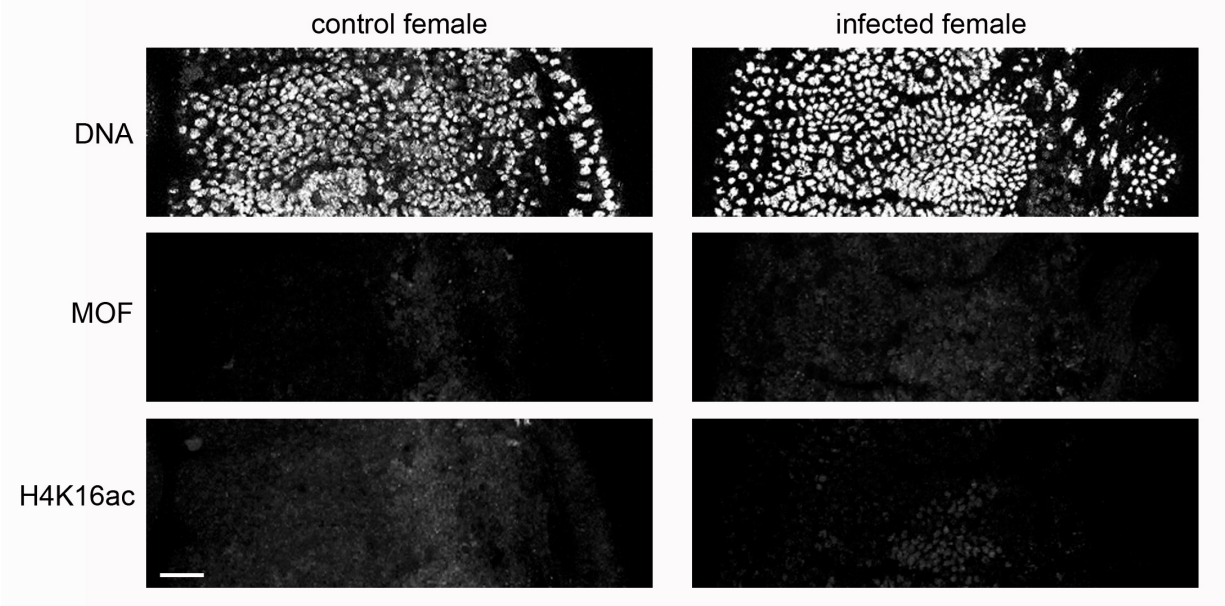

Figure S4

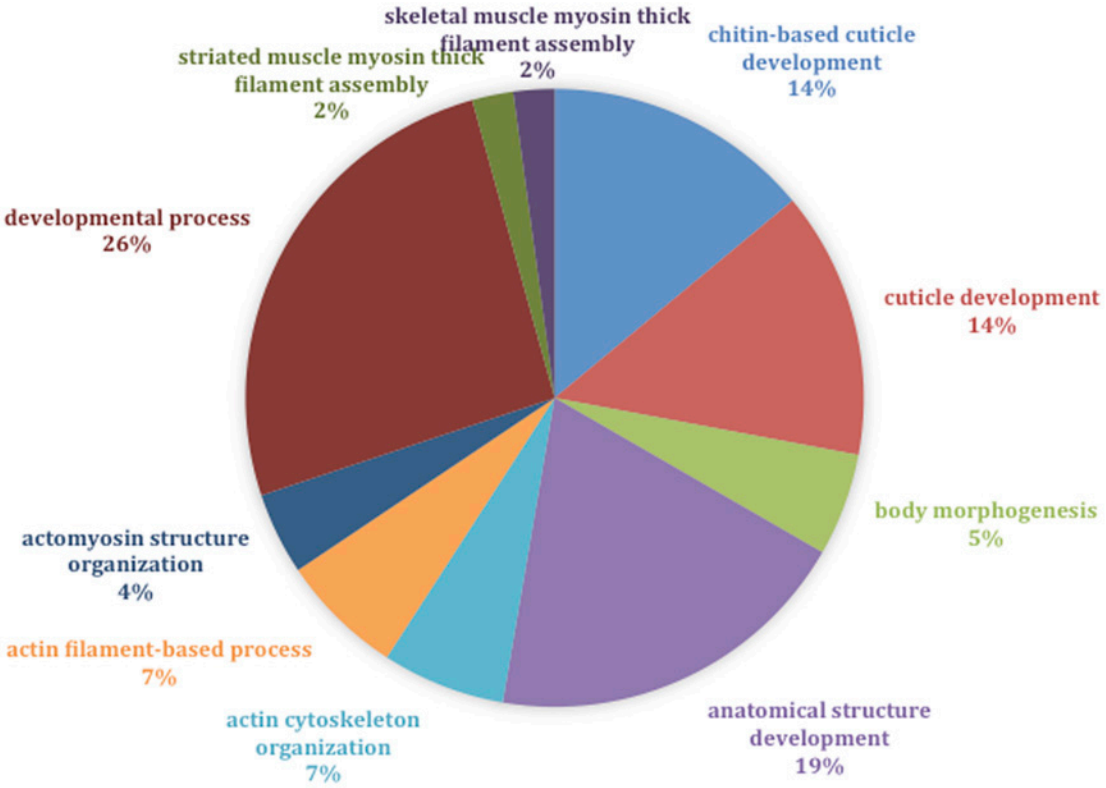

Figure S1. Localization patterns of MSL3-GFP and H4K16ac in uninfected and *Spiroplasma*-infected male embryos at 9-10hrs AED. In uninfected male embryos MSL3-GFP and H4K16ac co-localized to a single focus within each nucleus. In infected male embryos these signals were substantially reduced and highly irregular. Figure S1 is related to Figure 1.

Figure S2. H4K16ac foci in wild type male embryos correspond to X euchromatin. In uninfected embryos each nuclear region of X euchromatin, marked by a DNA FISH probe X16E, resides adjacent to or within a focus of H4K16ac. In *Spiroplasma*-infected embryos, H4K16ac signal is less intense and dispersed, and some X regions are not associated with this histone mark (red arrows). Scale bar equals 5 μm. Figure S2 is related to Figure 1.

Figure S3. Female embryos do not contain foci of MOF or H4K16ac. Female embryos were identified by the lack of signal from a Y-specific probe. Scale bar equals 15 μm. Figure S3 is related to Figure 1.

Figure S4. The biological functions of significantly mis-expressed genes that are common between both 2-3hr and 5-6hr developmental times. Seventy of these 72 genes making up the denominator of this analysis were over-expressed in the presence of *Spiroplasma*. This pie chart represents the top 10 gene ontology enrichments indicating the percentage of genes that are associated with each ontology type. Figure S4 is related to Figure 2.

Table S1. Gene expression data for control and Spiroplasma-infected embryos

Contents include (in appearing order): Mapping statistics; correlation matrix; raw FPKM and confidence intervals per sample; differential expression of all genes at 2-3hr; differential expression of all genes at 5-6hr; consistent genes; GO enrichment; results of

K-S Test. Table S1 is related to Figure 2. The data in Table S1 have been uploaded separately as an Excel Spreadsheet.

Supplemental Experimental Procedures

Transcriptional profiling

For analyzing gene expression patterns in *Spiroplasma*-infected male embryos, we created male enriched broods by using the segregation distortion (SD) system [S1]. Females of the genotype Rsp^S B^S *; SD-Mad / CyO*, which harbor an SD-sensitive responder locus that was translocated to the X chromosome, were crossed to males of the genotype X / Y ; SD-5 / CyO. The resulting male progeny, Rsp^S B^S */ Y ; SD-5 or SD-Mad / CyO*, were then crossed to *Spiroplasma*-infected females aged to one week and used for embryo collection.

Embryos were aged to either 2-3hrs or 5-6hrs AED at 25^{o}C, immediately flash frozen in liquid Nitrogen, and stored at -80^{o}C. A sample from each collection was fixed instead of flash freezing as described above and tested for sex ratio by using the Y chromosome-specific probe for FISH. The percentage of males ranged from 88% to 90% among collections. Total RNAs were extracted from previously frozen embryos using the Ambion mirVana mRNA isolation kit (Ambion/Applied Biosystems, Austin, TX). Extracted RNAs were treated with Ambion Turbo DNase (Ambion/Applied Biosystems, Austin, TX). The quality of RNA was assessed using the Bioanalyzer 2100 (Aglient Technologies, Santa Clara, CA) and the NanoDrop 1000 UV-VIS spectrophotometer (NanoDrop Technologies/Thermo Scientific, Wilmington, DE). RNA was then prepared for sequencing using the Illumina mRNA-Seq Sample Preparation Kit (Illumina San Diego, CA). The Illumina HiSeq 2000 sequencer was used for sequencing single-end–

sequenced libraries of either 50bp or 70bp in length (see Supplementary Table 1 for specifics). For each condition we analyzed two biological replicates of pooled, staged embryos.

Total polyA transcriptome reads per replicate for the uninfected 2-3hrs AED condition (23,951,431 and 23, 302,414 reads), infected 2-3hrs AED condition (27,341,453 and 36,736,297 reads), uninfected 5-6hrs AED condition (44,347,633 reads), and infected 5-6hrs AED condition (47,360,361 and 31,339,807 reads) were processed and aligned to a reference index generated for the *Drosophila melanogaster* genome BDGP5 (GCA_000001215.1) and transcriptome BDGP5.74 (both obtained from ftp.ensembl.org) using bowtie v1.0.0 and TopHat v2.0.10 [S2,3]. Reads were aligned using default parameters allowing up to 20 alignments per read with a maximum 2bp-mismatch. Quantification of annotated genes and isoforms was performed by Cufflinks v2.1.1 [S4]. Differential gene expression was analyzed using the cuffdiff module of Cufflinks. Hypergeometric tests for enrichment of genes with shared Biological Process Gene Ontology (GO) terms were performed using the online tool GOrilla [S5]. Sequence analysis, ratio distribution determinations, and Kolmogorov-Smirnov (K-S) tests were performed as previously described [S6,7]. The SRA accession number of the RNA sequences reported in this study is PRJNA318373.

Supplemental References

S1. Walker ES, Lyttle TW, Lucchesi JC (1989) Transposition of the Responder element (Rsp) of the Segregation distorter system (SD) to the X chromosome in Drosophila melanogaster. Genetics 122: 81-86.

S2. Langmead B, Trapnell C, Pop M, Salzberg SL (2009) Ultrafast and memory-efficient alignment of short DNA sequences to the human genome. Genome Biol 10: R25.

S3. Trapnell C, Pachter L, Salzberg SL (2009) TopHat: discovering splice junctions with RNA-Seq. Bioinformatics 25: 1105-1111.

S4. Trapnell C, Williams BA, Pertea G, Mortazavi A, Kwan G, et al. (2010) Transcript assembly and quantification by RNA-Seq reveals unannotated transcripts and isoform switching during cell differentiation. Nat Biotechnol 28: 511-515.
S5. Eden E, Navon R, Steinfeld I, Lipson D, Yakhini Z (2009) GOrilla: a tool for discovery and visualization of enriched GO terms in ranked gene lists. BMC Bioinformatics 10: 48.
S6. Sun L, Fernandez HR, Donohue RC, Li J, Cheng J, et al. (2013) Male-specific lethal complex in Drosophila counteracts histone acetylation and does not mediate dosage compensation. Proc Natl Acad Sci U S A 110: E808-817.
S7. Sun L, Johnson AF, Li J, Lambdin AS, Cheng J, et al. (2013) Differential effect of aneuploidy on the X chromosome and genes with sex-biased expression in Drosophila. Proc Natl Acad Sci U S A 110: 16514-16519.